Eur. Phys. J. D **40**, 223–230 (2006)
DOI: 10.1140/epjd/e2006-00159-2

THE EUROPEAN PHYSICAL JOURNAL D

Cross-section and rate coefficient calculation for electron impact excitation, ionisation and dissociation of H_2 and OH molecules

R. Riahi[1], Ph. Teulet[2,a], Z. Ben Lakhdar[1], and A. Gleizes[2]

[1] Laboratoire de Spectroscopie Atomique, Moléculaire et Applications, Département de Physique, Faculté des Sciences de Tunis, Université de Tunis el Manar, 1060 Tunis, Tunisia
[2] Centre de Physique des Plasmas et Applications de Toulouse, UMR CNRS 5002, Université Paul Sabatier Toulouse 3, 118 route de Narbonne, 31062 Toulouse Cedex 09, France

Received 14 February 2006 / Received in final form 2 June 2006

Abstract. The weighted total cross-section (WTCS) theory is used to calculate electron impact excitation, ionisation and dissociation cross-sections and rate coefficients of OH, H_2, OH^+, H_2^+, OH^- and H_2^- diatomic molecules in the temperature range 1500–15000 K. Calculations are performed for H_2(X, B, C), OH(X, A, B), H_2^+(X), OH^+(X, a, A, b, c), H_2^-(X) and OH^-(X) electronic states for which Dunham coefficients are available. Rate coefficients are calculated from WTCS assuming Maxwellian energy distribution functions for electrons and heavy particles. One and two temperature (θ_e and θ_g respectively for electron and heavy particles kinetic temperatures) results are presented and fitting parameters (a, b and c) are given for each reaction rate coefficient: $k(\theta) = a(\theta^b)\exp(-c/\theta)$.

PACS. 52.20.-j Elementary processes in plasmas – 52.20.Fs Electron collisions – 82.33.Xj Plasma reactions

1 Introduction

Controlling or restoring water quality are major steps for environment preservation and sustainable development. Numerous fields of industrial activities are concerned with the elimination of toxic organic molecules or with the detection of hazardous metallic pollutants of waste water. Plasma processes can be used for these tasks and there are many works dealing with trace elements analysis or contaminants detection in aqueous solutions using Laser Induced Breakdown Spectroscopy (LIBS) techniques [1–8]. There are also several studies concerning the treatment and the decontamination of spoiled waste water using radiofrequency (RF) plasma [9] or DC torches [10]. In these applications, the destruction of organic molecules takes place through chemical reactions where the OH radical plays a key role. For a better understanding of the chemistry occurring in such plasma devices, it is necessary to have reliable sets of cross-sections and rate coefficients of the chemical reactions involving the diatomic molecules OH and H_2 resulting from the decomposition of water. These data are also essential to undertake the development of hydro-kinetic or collisional-radiative models of LIBS plasma expansion [11,12].

In the present study, electron impact excitation, ionisation and dissociation of OH and H_2 electronic states and the corresponding ions are investigated. The weighted total cross-section (WTCS) theory [13] applied initially to air molecules [14–17] and recently re-examined and improved by Teulet et al. [18] is used to calculate inelastic collision cross-sections. Reaction rate coefficients are then determined assuming Maxwellian energy distribution functions for electrons and heavy particles. In the case of LIBS plasma, these assumptions become valid after the initial formation phase (i.e. some hundred nanoseconds after the laser pulse).

There is to our knowledge no reaction rate coefficient values published for electron impact excitation, ionisation or dissociation of OH. The only available data are ionisation cross-sections for the process: OH(X) + e → OH^+(X) + e + e [19–22]. For reaction rate coefficients involving H_2 molecules, the works of Janev et al. [23], Du and Hessler [24] and Celiberto et al. [25] can be mentioned. Janev et al. [23] published a compilation of rate coefficients for electron impact excitation (H_2X → B and X → C), ionisation (H_2X → H_2^+X) and dissociation (H_2X). Du and Hessler [24] studied the dissociation of H_2(X). They proposed a temperature dependent rate coefficient determined experimentally by least-squares analysis of measured absorption profiles. Celiberto et al. [25] calculated the excitation rate coefficient (H_2(X, $v = 0$) → H_2(C)) from electron impact cross-sections in the frame of the impact-parameter method. On the other hand, it exists relatively large sets of cross-sections data for the e-H_2 system. Concerning electron impact excitation (H_2X → B and X → C), the works of Chung and Lin [26], Khakoo and Trajmar [27], Mu-Tao et al. [28], Khare [29], Arrighini

---

[a] e-mail: `teulet@cpat.ups-tlse.fr`

Table 1. Spectroscopic constants of H_2, H_2^+ and H_2^- electronic states.

State	T_e (cm^{-1})	ω_e (cm^{-1})	$\omega_e x_e$ (cm^{-1})	$\omega_e y_e$ (cm^{-1})	r_e (10^{-8} cm)	D_0 (cm^{-1})
$H_2^+ X\ ^2\Sigma_g^+$	124420	2323.23	67.39	0.93	1.057	21380.0
$H_2 C\ ^1\Pi_u$	100089.8	2443.77	69.524	0.7312	1.033	19784.4
$H_2 B\ ^1\Sigma_u^+$	91700.0	1358.09	20.888		1.293	28174.2
$H_2 X\ ^1\Sigma_g^+$	0.0	4403.566	123.8573	1.87269	0.741	36118.3
$H_2^- X\ ^1\Sigma_g^+$	−8778.86	1700	35.0		1.150	9864.0

Table 2. Spectroscopic constants of OH, OH^+ and OH^- electronic states.

State	T_e (cm^{-1})	ω_e (cm^{-1})	$\omega_e x_e$ (cm^{-1})	$\omega_e y_e$ (cm^{-1})	r_e (10^{-8} cm)	D_0 (cm^{-1})
$OH^+ c\ ^1\Sigma^+$	148196.64	1797.30	52.400		1.2258	12116.6
$OH^+ b\ ^1\Sigma^+$	133616.54	3120.00	79.950		1.0331	26696.7
$OH^+ A\ ^3\Pi_i$	132484.04	2133.65	79.550		1.1354	12114.7
$OH^+ a\ ^1\Delta$	121701.54	3143.00	72.750		1.0335	38611.7
$OH^+ X\ ^3\Sigma^-$	104045.54	3113.37	78.515		1.0289	40400.0
$OHB\ ^2\Sigma^+$	68372.0	940.00	105.000	−21.500	1.86980	870.4
$OHA\ ^2\Sigma^+$	32684.1	3178.86	92.917	−1.7915	1.01210	18633.6
$OHX\ ^2\Pi_i$	0.0	3737.76	84.881	0.5409	0.96966	35450.0
$OH^- X\ ^1\Sigma^+$	−14722.84	3800.00	88.00		0.9628	38351.0

et al. [30] and Celiberto and Rescigno [31] can be mentioned. For ionisation ($H_2X \rightarrow H_2^+X$), we should consider the papers of Krishnakumar and Srivastava [32], Rapp and Englander-Golden [33], Deutsch et al. [34], Straub et al. [35] and Dose et al. [36]. Moreover, reference should be made to the review (excitation $H_2X \rightarrow B$ and $X \rightarrow C$, ionisation $H_2X \rightarrow H_2^+X$ and dissociation of H_2^+) by Tawara et al. [37] and it is also necessary to point out the compilation of theoretical cross-sections collected for electron impact excitation and ionisation by Celiberto et al. [38].

This bibliographic survey shows clearly a lack of data in particular with regard to OH molecule. As a consequence, it seems essential to calculate a complete and reliable set of electron impact inelastic cross-sections and reaction rate coefficients for OH, H_2 and their corresponding ions before undertaking a collisional-radiative or an hydro-kinetic modelling of water plasma.

2 WTCS theory

The method of calculation of electron impact cross-sections is not presented in details in this work. A fully description of the WTCS theory could be find in previous works [13,18].

An energy level belonging to a particular molecular state is characterized by its electronic energy term T_e and its vibrational and rotational quantum numbers v and J. The potential energy $U(T_e,\ v,\ J,\ r)$ of each electronic state is defined by the well-known Morse's potential function [39] where r is the internuclear separation.

Dunham coefficients necessary to implement the calculation of cross-sections are given in Tables 1 and 2 for the considered molecular electronic states of H_2, H_2^+ and H_2^-, and OH, OH^+ and OH^- respectively [40–43].

Assuming that vibrational and rotational temperatures are respectively equal to electron ($\theta_v = \theta_e$) and heavy particles ($\theta_r = \theta_g$) temperatures [18], the WTCS for a transition between an initial level T_1 to a final state T_2 is given by:

$$Q_{T_1}^{T_2}(\varepsilon, \theta_e, \theta_g) = \sum_{v_1=0}^{v_L(T_1)} P(v_1, \theta_e) \sum_{J_1=0}^{J_L(v_1)} P(J_1, \theta_g) \times \int_0^\infty P_{v_1}(r) \sum_{v_2=0}^{v_L(T_2)} \sum_{J_2=0}^{J_L(v_2)} q_{T_1,v_1,J_1}^{T_2,v_2,J_2}(r,\varepsilon) dr \quad (1)$$

where ε is the energy of the incoming electron and $q_{T_1,v_1,J_1}^{T_2,v_2,J_2}(r,\varepsilon)$ the elementary cross-section corresponding to a transition between a stable rovibrational level of the electronic state T_1 and a stable rovibrational level of T_2 (excitation or ionisation) or an unstable one (dissociation). $v_L(T_i)$ and $J_L(T_i,\ v_i)$ are respectively the maximum values of the vibrational quantum number of the electronic state T_i and of the rotational quantum number of the electro-vibrational level (T_i, v_i). v_L and J_L are determined with the Morse's potential function minimisation method [44]. $P(v_1,\ \theta_e)$, $P(J_1,\ \theta_g)$ and $P_{v1}\ (r)$ are respectively: (i) the probability for the molecule to be at the temperature θ_e in the vibrational level v_1 of the electronic state T_1, (ii) the probability for the molecule to be at the temperature θ_g in the rotational level J_1 of the electro-vibrational state (T_1, v_1) and (iii) the probability for the internuclear separation to be in the range r, $r + dr$. The product of $P(v_1,\ \theta_e)$ and $P(J_1, \theta_g)$ is given by [18]:

$$P(v_1, \theta_e) P(J_1, \theta_g) = \frac{1}{Z(T_1, \theta_e, \theta_g)} (2J_1 + 1) \times \exp\left(-\frac{G(v_1)}{k\theta_e}\right) \exp\left(-\frac{F_{v_1}(J_1)}{k\theta_g}\right) \quad (2)$$

where k is the Boltzmann constant. $G(v_1)$, $F_{v_1}(J_1)$ and $Z(T_1,\ \theta_e,\ \theta_g)$ are respectively vibrational energy,

Table 3. Normalization coefficients for excitation and ionisation processes of H$_2$ and H_2^+.

Type of transition	Transitions	References	Calculated α_{g1g2}	Used α_{g1g2}
singlet-singlet	$\mathrm{H_2\ X\ ^1\Sigma_g^+ \rightarrow H_2\ B^1\Sigma_u^+}$	[26,27,29,31,37,38]	$4 \times 10^{-1(a)}$	$\alpha_{11} = 4 \times 10^{-1}$
	$\mathrm{H_2\ X\ ^1\Sigma_g^+ \rightarrow H_2\ C^1\Pi_u}$	[27–31,37,38]	$4 \times 10^{-1(a)}$	
	$\mathrm{H_2\ B^1\Sigma_u^+ \rightarrow H_2\ C^1\Pi_u}$	–	–	
singlet-doublet	$\mathrm{H_2\ X\ ^1\Sigma_g^+ \rightarrow H_2^+\ X\ ^2\Sigma_g^+}$	[32–36,38]	10^{-2}	$\alpha_{12} = 10^{-2}$
	$\mathrm{H_2\ B^1\Sigma_u^+,\ H_2\ C^1\Pi_u \rightarrow H_2^+\ X\ ^2\Sigma_g^+}$	–	–	

[(a)] α_{g1g2} was finally determined from [27] because cross-sections given by these authors are experimental results.

rotational energy and two-temperature internal partition function of the electronic state T_1. These terms are calculated from spectroscopic constants given in Tables 1 and 2 according to references [13,18].

The probability $P_{v1}(r)$ is calculated within the assumption of the harmonic oscillator. This hypothesis implies that $P_{v1}(r)$ depends only on the internuclear distance r and on the vibrational quantum number v_1 [39]:

$$P_{v_1}(r) = \frac{1}{2^{v_1} v_1!} \sqrt{\frac{\alpha}{\pi}} \exp(-\alpha(r - r_e)^2) H_{v_1}^2(\chi) \qquad (3)$$

with $\chi = \sqrt{\alpha}(r - r_e)$, $\alpha = (2\pi/h)\sqrt{\mu k_0}$ and $k_0 = 4\pi^2 c^2 \mu \omega_e^2$. c is the speed of light, h is Planck constant, μ is the reduced mass of the molecule, r_e is the equilibrium internuclear distance and H_{v1} is the Hermitian polynomial of the v_1th degree.

For electron impact excitation and ionisation, the WTCS is finally given by:

$$\begin{aligned} Q_{T_1}^{T_2}(\varepsilon, \theta_e, \theta_g) &= \frac{1}{Z(T_1, \theta_e, \theta_g)} \sum_{v_1=0}^{v_L(T_1)} \exp\left(-\frac{G(v_1)}{k\theta_e}\right) \\ &\times \sum_{J_1=0}^{J_L(v_1)} (2J_1 + 1) \exp\left(-\frac{F_{v_1}(J_1)}{k\theta_g}\right) \\ &\times \sum_{v_2=0}^{v_L(T_2)} \sum_{J_2=0}^{J_L(v_2)} \delta_{(J_2, J_1 \pm 2)} \int_0^\infty P_{v_1}(r)\, q_{T_1, v_1, J_1}^{T_2, v_2, J_2}(r, \varepsilon) dr. \qquad (4) \end{aligned}$$

$\delta_{(J_2, J_{1\pm2})}$ is the Kronecker's symbol introduced in the calculation in order to respect selection rules ($J_2 = J_1 \pm 2$) established by Stein and Gerjuoy [45] for transitions between rotational levels. In this case, the elementary cross-section $q_{T_1,v_1,J_1}^{T_2,v_2,J_2}(r, \varepsilon)$ is taken from Drawin [18,46]. Calculations are performed according to the Franck and Condon principle: an electron-molecule collision leading to a transition between a state (T_1, v_1, J_1) to another one (T_2, v_2, J_2) is supposed to be fast enough so that this transition occurs at constant internuclear distance. It is also necessary to define stability areas for each electronic level to undertake WTCS calculations. Stability areas used in this work are the one defined by Teulet et al. [18] to avoid undesirable dissociative excitation processes.

For dissociation processes, the WTCS is calculated with:

$$\begin{aligned} Q_{T_1}^{D}(\varepsilon, \theta_e, \theta_g) &= \frac{1}{Z(T_1, \theta_e, \theta_g)} \sum_{v_1=0}^{v_L(T_1)} \exp\left(-\frac{G(v_1)}{k\theta_e}\right) \\ &\times \sum_{J_1=0}^{J_L(v_1)} (2J_1 + 1) \exp\left(-\frac{F_{v_1}(J_1)}{k\theta_g}\right) \\ &\times \int_0^\infty P_{v_1}(r)\, q_{T_1, v_1, J_1}^{D}(r, \varepsilon) dr. \qquad (5) \end{aligned}$$

In this case, the elementary cross-section $q_{T_1,v_1,J_1}^{D}(r, \varepsilon)$ is obtained according to Gryzinski's formalism [18,47]. Calculation assumptions are the same as for excitation and ionisation processes but the rotational predissociation phenomenon (see Herzberg [39]) is also taken into account: stability areas of each electronic state are modified [18] to avoid possible transitions leading to undesirable predissociation of the final rotational level after the collision which do not have to be considered in the calculation of the total dissociation cross-section.

For electron impact excitation and ionisation, the elementary cross-section $q_{T_1,v_1,J_1}^{T_2,v_2,J_2}(r, \varepsilon)$ taken from Drawin [46] requires the determination of dimensionless normalisation factors α_{g1g2} ($g_1 = 2S_1 + 1$ and $g_2 = 2S_2 + 1$ are respectively spin multiplicities of the initial and final electronic levels T_1 and T_2 of the transition). These coefficients can be evaluated by comparing WTCS calculated at 300 K with available experimental cross-sections. Unfortunately, for most of electronic transitions, it does not exist published data allowing to calculate normalisation factors. In these cases, α_{g1g2} coefficients can be deduced from other α_{g1g2} values (determined with available experimental data) according to the following assumptions:

– hypothesis 1: transitions occur without change of spin multiplicity $\Delta S = 0$ ($g_1 = g_2$);
– hypothesis 2: transitions occur without change of spin multiplicity for the final state ($\alpha_{g3g2} = \alpha_{g1g2}$).

Normalisation factors α_{g1g2} used in this work are summarised in Tables 3 and 4 for H$_2$ and OH respectively.

Finally, assuming Maxwellian energy distribution functions for all chemical species of the plasma, the knowledge of normalised WTCS allows to calculate two

Table 4. Normalization coefficients for excitation and ionisation processes of OH and OH^+.

Type of transition	Transitions	References	Calculated α_{g1g2}	Used α_{g1g2}
singlet-singlet	$OH^+\ a^1\Delta \rightarrow OH^+\ b^1\Sigma^+$, $OH^+\ c^1\Sigma^+$	–	–	$\alpha_{11} = 1^{(a)}$
doublet-doublet	$OH\ X\ ^2\Pi_i \rightarrow OH\ A^2\Sigma^+$, $OH\ B^2\Sigma^+$	–	–	$\alpha_{22} = 1^{(a)}$
	$OH\ A^2\Sigma^+ \rightarrow OH\ B^2\Sigma^+$	–		
doublet-triplet	$OH\ X\ ^2\Pi_i \rightarrow OH^+\ X^3\Sigma^-$	[19–22]	$\alpha_{23} = 10^{-2}$	$\alpha_{23} = 10^{-2}$
	$OH\ A^2\Sigma^+$ $OH\ B^2\Sigma^+ \rightarrow OH^+\ X^3\Sigma^-$	–	–	
	$OH\ X\ ^2\Pi_i$, $OH\ A^2\Sigma^+$, $OH\ B^2\Sigma^+ \rightarrow OH^+\ A^3\Pi_i$	–	–	
doublet-singlet	$OH\ X\ ^2\Pi_i$, $OH\ A^2\Sigma^+$,$OH\ B^2\Sigma^+ \rightarrow OH^+\ a^1\Delta$, $OH^+\ b^1\Sigma^+$, $OH^+\ c^1\Sigma^+$	–	–	$\alpha_{21} = 1^{(a)}$
triplet-singlet	$OH^+\ X^3\Sigma^- \rightarrow OH^+\ a^1\Delta$, $OH^+\ b^1\Sigma^+$, $OH^+\ c^1\Sigma^+$	–	–	$\alpha_{31} = 1^{(a)}$
singlet-triplet	$OH^+\ a^1\Delta \rightarrow OH^+\ A^3\Pi_i$	–	hypothesis 2 $\alpha_{13} = \alpha_{23}$	$\alpha_{13} = 10^{-2}$
triplet-triplet	$OH^+\ X^3\Sigma^- \rightarrow OH^+\ A^3\Pi_i$	–	–	$\alpha_{33} = 1^{(a)}$

(a) Due to the lack of data for these transitions, it was not possible to obtain normalisation factors. α_{g1g2} coefficients were finally fixed to 1. They will have to be modified if new experimental cross-sections are published in the future.

Table 5. Fitting coefficients for electron impact dissociation ($k(\mathrm{cm}^3\ \mathrm{s}^{-1}) = a\theta^b \exp(-c/\theta)$ with θ in Kelvin).

State	a	b	c (K)	State	a	b	c (K)
H_2 X	4.47×10^{-4}	–0.80	126564.9	OH B	1.35×10^{-2}	–1.43	11320.7
H_2 B	6.57×10^{-4}	–1.05	69092.0	OH^+X	$3.19 \times 10^{+4}$	–2.04	175461.8
H_2 C	$8.12 \times 10^{+2}$	–2.57	48589.9	OH^+a	$7.22 \times 10^{+3}$	–2.01	152189.9
H_2^+ X	6.34×10^{-4}	–0.87	80265.1	OH^+A	9.38×10^{-2}	–0.81	57020.8
H_2^- X	1.36×10^{-3}	–0.81	45444.1	OH^+b	$4.10 \times 10^{+4}$	–2.12	117593.5
OH X	2.55×10^{-4}	–0.76	80107.4	OH^+c	$1.13 \times 10^{+4}$	–2.18	59479.1
OH A	1.72×10^{-4}	–0.75	45277.3	OH^- X	$4.65 \times 10^{+2}$	–1.89	140376.8

Table 6. Fitting coefficients for electron impact excitation of H_2 ($k(\mathrm{cm}^3\ \mathrm{s}^{-1}) = a\theta^b\ \exp(-c/\theta)$ with θ in Kelvin).

State	a	b	c (K)
H_2 X → H_2 B	1.79×10^{-15}	1.66	173307.5
H_2 X → H_2 C	1.14×10^{-14}	1.17	173411.2
H_2 B → H_2 C	3.67×10^{-08}	–0.26	34769.1

temperature reaction rate coefficients as:

$$k_{T_1}^{T_2}(\theta_e, \theta_g) = 2\left(\frac{2}{\pi m_e}\right)^{0.5} (k\theta_e)^{-1.5} \times \int_0^\infty \varepsilon Q_{T_1}^{T_2}(\varepsilon, \theta_e, \theta_g) \exp\left(-\frac{\varepsilon}{k\theta_e}\right) d\varepsilon \quad (6)$$

where m_e is the electron mass.

3 Results and discussions

Reaction rate coefficients were first calculated as a function of temperature in thermal equilibrium conditions ($\theta = \theta_e = \theta_g$) and were fitted in an Arrhenius form: $k(\mathrm{cm}^3\,\mathrm{s}^{-1}) = a(\theta^b) \exp(-c/\theta)$ in the range 1500–15000 K. Fitting coefficients a, b and c are given in Table 5 for dissociation. They are summarised in Tables 6 and 7 for electron impact excitation of H_2 and OH and OH^+ respectively and in Tables 8 and 9 for ionisation of H_2 and OH respectively.

Table 7. Fitting coefficients for electron impact excitation of OH and OH^+ ($k(\mathrm{cm}^3\ \mathrm{s}^{-1}) = a\theta^b \exp(-c/\theta)$ with θ in Kelvin).

State	a	b	c (K)
OH X→ OH A	1.17×10^{-8}	0.52	44642.8
OH X→ OH B	1.11×10^{-24}	4.10	98540.8
OH A→ OH B	9.00×10^{-20}	2.76	54911.4
OH^+ X → OH^+ a	8.53×10^{-12}	0.83	19995.5
OH^+ X → OH^+ A	1.18×10^{-9}	0.49	37523.1
OH^+ X → OH^+ b	1.98×10^{-10}	0.68	39547.9
OH^+ X → OH^+ c	1.33×10^{-11}	1.00	58016.5
OH^+ a → OH^+ A	5.87×10^{-17}	1.94	1796.3
OH^+ a → OH^+ b	1.45×10^{-7}	–0.33	24371.1
OH^+ a → OH^+ c	6.07×10^{-12}	0.81	36573.5
OH^+ A → OH^+ b	4.09×10^{-9}	2.71	15586.8
OH^+ A → OH^+ c	1.66×10^{-7}	–0.27	28184.8
OH^+ b → OH^+ c	1.75×10^{-9}	0.17	22776.9

Reaction rate coefficients were also calculated in the two-temperature case ($\theta_e \neq \theta_g$) in the range 1500–15000 K. As examples, rate coefficients of the three following processes:

$$H_2(X) + e^- \rightarrow H_2(C) + e^-$$

$$OH(X) + e^- \rightarrow OH(A) + e^-$$

$$OH(X) + e^- \rightarrow OH^+(X) + e^- + e^-$$

are shown in Tables 10, 11 and 12 respectively. We can see from these results that the dependence on θ_g is weak

Table 8. Fitting coefficients for electron impact ionisation of H_2 ($k(\mathrm{cm}^3\ \mathrm{s}^{-1}) = a\theta^b \exp(-c/\theta)$ with θ in Kelvin).

State	a	b	c (K)
H_2 X → H_2^+ X	2.96×10^{-15}	1.61	207639.4
H_2 B → H_2^+ X	2.71×10^{-11}	0.92	79581.8
H_2 C → H_2^+ X	1.01×10^{-12}	1.23	45162.5

Table 9. Fitting coefficients for electron impact ionisation of OH ($k(\mathrm{cm}^3\ \mathrm{s}^{-1}) = a\theta^b \exp(-c/\theta)$ with θ in Kelvin).

State	a	b	c (K)
OH X → OH^+ X	1.16×10^{-17}	1.78	160267.1
OH X → OH^+ a	6.35×10^{-17}	2.06	184211.0
OH X → OH^+ A	2.52×10^{-12}	0.55	197451.2
OH X → OH^+ b	3.79×10^{-14}	1.45	195693.9
OH X → OH^+ c	6.53×10^{-15}	1.61	218785.3
OH A → OH^+ X	7.44×10^{-22}	2.61	122729.2
OH A → OH^+ a	$1.32{\times}10^{-13}$	1.15	162260.8
OH A → OH^+ A	1.23×10^{-8}	–0.37	163688.3
OH A → OH^+ b	$5.42{\times}10^{-12}$	0.83	162235.8
OH A → OH^+ c	2.27×10^{-12}	0.87	173229.1
OH B → OH^+ X	4.56×10^{-9}	–0.31	125413.6
OH B → OH^+ a	2.35×10^{-5}	–0.74	160772.7
OH B → OH^+ A	5.75×10^{-12}	0.36	135657.8
OH B → OH^+ b	5.69×10^{-5}	–0.81	149261.0
OH B → OH^+ c	1.39×10^{-6}	–0.48	160416.5

compared to the variation with θ_e. As it was not feasible to expose here all the two-temperature reaction rate coefficients, these data could be obtained from the authors upon request. Finally, it was not possible to compare our two-temperature results with previous data because, to our knowledge, there are no available multi-temperature reaction rate coefficients for H_2 and OH molecules in the literature.

On the other hand, 300 K WTCS and one temperature rate coefficients calculated in this study can be compared with former theoretical or experimental works. Concerning cross-sections, we have compared our results with published values in Figures 1–4 respectively for the following processes:

$$H_2(\mathrm{X}) + e^- \rightarrow H_2(\mathrm{C}) + e^-$$
$$H_2(\mathrm{X}) + e^- \rightarrow H_2^+(\mathrm{X}) + e^- + e^-$$
$$\mathrm{OH(X)} + e^- \rightarrow \mathrm{OH}^+(\mathrm{X}) + e^- + e^-$$
$$H_2^+(\mathrm{X}) + e^- \rightarrow \mathrm{H}^+ + \mathrm{H} + e^-.$$

For the excitation process H_2(X) → H_2(C) (cf. Fig. 1), the general behaviour of our cross-section is similar (threshold energy and position of the maximum) to the previous theoretical results of Mu-Tao et al. [28], Khare [29] and Celiberto and Rescigno [31]. The agreement is obviously good with the experimental cross-sections of Khakoo and Trajmar [27] because the H_2(X) → H_2(C) WTCS calculated in this work is normalised with these data. For electron impact ionisation of H_2(X) and OH(X), the shape of the cross-sections obtained in this study is the same as the one of former works for H_2 [32–35] and OH [19–22]

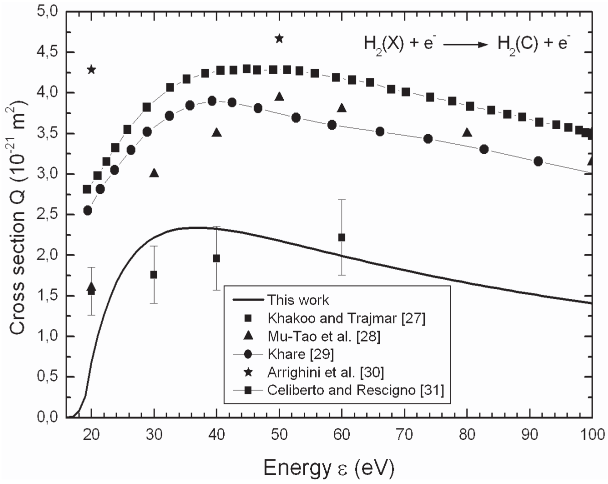

Fig. 1. Comparison between 300 K WTCS and published cross-sections for electron impact excitation of H_2(X → C).

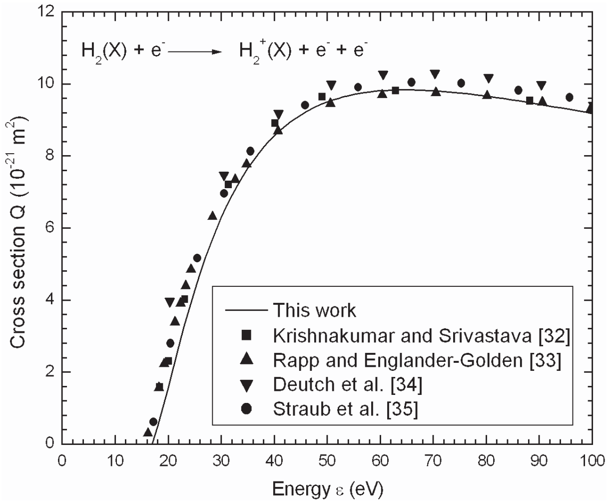

Fig. 2. Comparison between 300 K WTCS and previous cross-sections for electron impact ionisation of H_2(X).

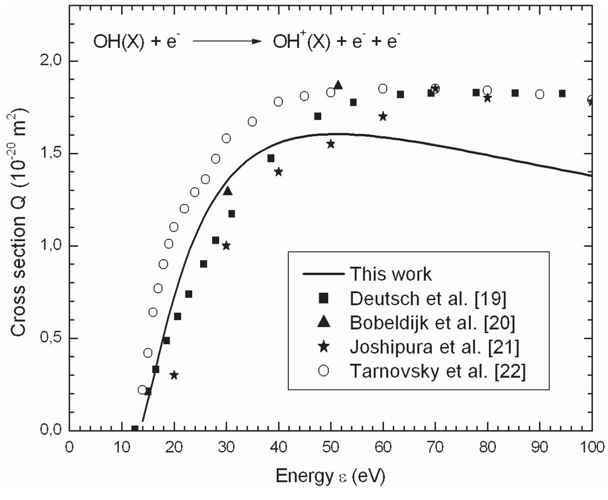

Fig. 3. Comparison between 300 K WTCS and published cross-sections for electron impact ionisation of OH(X).

Table 10. Excitation rate coefficients (cm^3 s^{-1}) for $H_2(X) \rightarrow H_2(C\ ^1\Pi_u)$.

	θ_g (K)						
θ_e (K)	2000	4000	6000	8000	10000	12000	14000
2000	1.885×10^{-48}	1.825×10^{-48}	1.754×10^{-48}	1.626×10^{-48}	1.430×10^{-48}	1.178×10^{-48}	4.409×10^{-48}
4000	2.904×10^{-29}	2.860×10^{-29}	2.750×10^{-29}	2.552×10^{-29}	2.248×10^{-29}	1.864×10^{-29}	1.532×10^{-29}
6000	9.517×10^{-23}	9.001×10^{-23}	8.689×10^{-23}	8.104×10^{-23}	7.194×10^{-23}	6.057×10^{-23}	5.095×10^{-23}
8000	1.942×10^{-19}	1.833×10^{-19}	1.780×10^{-19}	1.673×10^{-19}	1.501×10^{-19}	1.285×10^{-19}	1.105×10^{-19}
10000	2.088×10^{-17}	1.975×10^{-17}	1.928×10^{-17}	1.827×10^{-17}	1.659×10^{-17}	1.442×10^{-17}	1.264×10^{-17}
12000	5.180×10^{-16}	4.876×10^{-16}	4.787×10^{-16}	4.568×10^{-16}	4.192×10^{-16}	3.699×10^{-16}	3.292×10^{-16}
14000	4.946×10^{-15}	4.930×10^{-15}	4.877×10^{-15}	4.684×10^{-15}	4.337×10^{-15}	3.873×10^{-15}	3.493×10^{-15}

Table 11. Excitation rate coefficients (cm^3 s^{-1}) for $OH(X) \rightarrow OH(A\ ^2\Sigma^+)$.

	θ_g (K)						
θ_e (K)	2000	4000	6000	8000	10000	12000	14000
2000	1.321×10^{-16}	1.303×10^{-16}	1.280×10^{-16}	1.254×10^{-16}	1.227×10^{-16}	1.204×10^{-16}	1.185×10^{-16}
4000	1.352×10^{-11}	1.340×10^{-11}	1.319×10^{-11}	1.294×10^{-11}	1.267×10^{-11}	1.243×10^{-11}	1.223×10^{-11}
6000	6.969×10^{-10}	6.929×10^{-10}	6.853×10^{-10}	6.745×10^{-10}	6.620×10^{-10}	6.496×10^{-10}	6.391×10^{-10}
8000	5.225×10^{-9}	5.218×10^{-9}	5.183×10^{-9}	5.125×10^{-9}	5.047×10^{-9}	4.963×10^{-9}	4.891×10^{-9}
10000	1.814×10^{-8}	1.796×10^{-8}	1.792×10^{-8}	1.779×10^{-8}	1.760×10^{-8}	1.737×10^{-8}	1.717×10^{-8}
12000	4.274×10^{-8}	4.506×10^{-8}	4.156×10^{-8}	4.143×10^{-8}	4.114×10^{-8}	4.079×10^{-8}	4.045×10^{-8}
14000	7.786×10^{-8}	7.707×10^{-8}	7.661×10^{-8}	7.634×10^{-8}	7.630×10^{-8}	7.596×10^{-8}	7.530×10^{-8}

Table 12. Ionisation rate coefficients (cm^3 s^{-1}) for $OH(X) + e \rightarrow OH^+(X\ ^3\Sigma^-) + e + e$.

	θ_g (K)						
θ_e (K)	2000	4000	6000	8000	10000	12000	14000
2000	1.381×10^{-46}	1.362×10^{-46}	1.338×10^{-46}	1.310×10^{-46}	1.282×10^{-46}	1.258×10^{-46}	1.238×10^{-46}
4000	1.205×10^{-28}	1.193×10^{-28}	1.173×10^{-28}	1.150×10^{-28}	1.126×10^{-28}	1.104×10^{-28}	1.089×10^{-28}
6000	1.581×10^{-22}	1.569×10^{-22}	1.550×10^{-22}	1.523×10^{-22}	1.494×10^{-22}	1.467×10^{-22}	1.443×10^{-22}
8000	2.106×10^{-19}	2.099×10^{-19}	2.082×10^{-19}	2.056×10^{-19}	2.024×10^{-19}	1.993×10^{-19}	1.967×10^{-19}
10000	1.744×10^{-17}	1.717×10^{-17}	1.712×10^{-17}	1.698×10^{-17}	1.681×10^{-17}	1.662×10^{-17}	1.648×10^{-17}
12000	3.411×10^{-16}	3.406×10^{-16}	3.401×10^{-16}	3.389×10^{-16}	3.382×10^{-16}	3.362×10^{-16}	3.352×10^{-16}
14000	4.060×10^{-15}	3.865×10^{-15}	3.681×10^{-15}	3.496×10^{-15}	3.304×10^{-15}	3.101×10^{-15}	2.981×10^{-15}

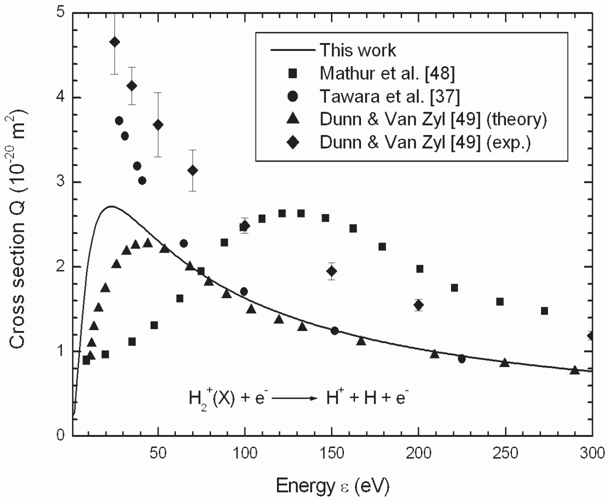

Fig. 4. Comparison between 300 K WTCS and published cross-sections for electron impact dissociation of $H_2^+(X)$.

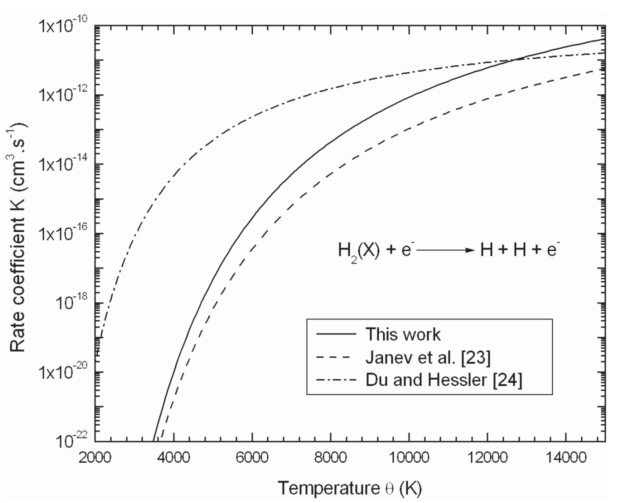

Fig. 5. Comparison between our rate coefficient and published values for electron impact dissociation of $H_2(X)$.

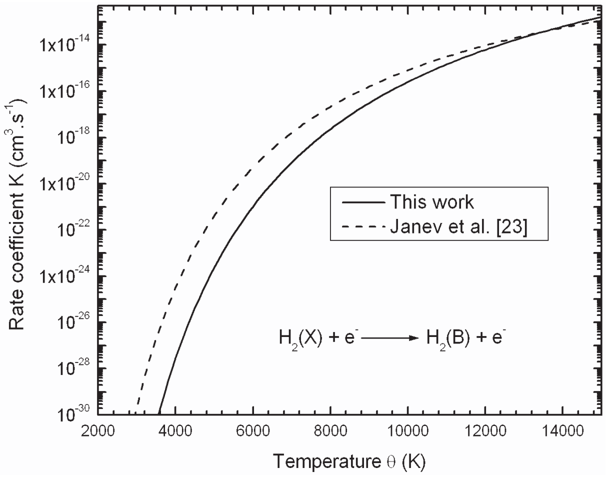

Fig. 6. Comparison between our rate coefficient and published values for electron impact excitation of H_2(X → B).

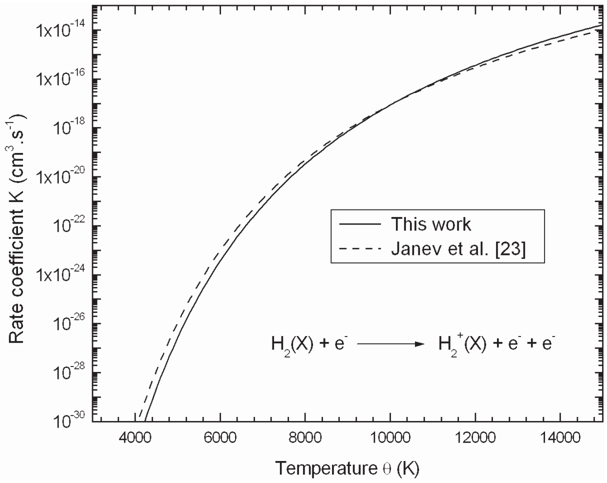

Fig. 8. Comparison between our rate coefficient and published values for electron impact ionisation of H_2(X).

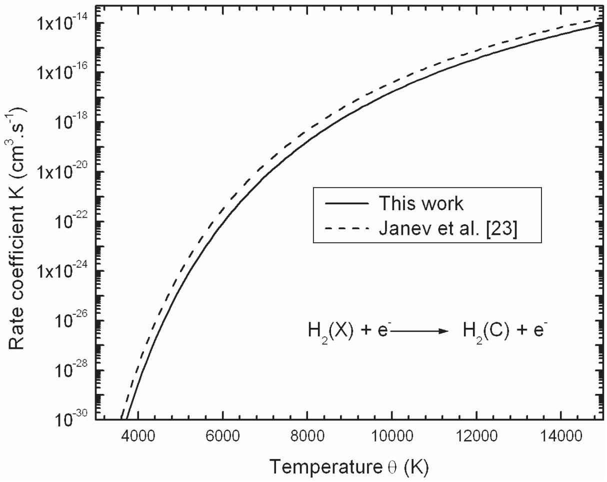

Fig. 7. Comparison between our rate coefficient and published values for electron impact excitation of H_2(X → C).

(cf. Figs. 2 and 3). For the dissociation of H_2^+(X), the WTCS is compared in Figure 4 with previous published theoretical [49] and experimental [37,48,49] works. It should be noted that our cross-sections are not normalised with experimental value in the case of dissociation. The agreement between our results and the theoretical data of Dunn and Van Zyl [49] is acceptable but there are more discrepancies mainly at low energy with the measured cross-sections of Tawara et al. [37], Mathur et al. [48] and Dunn and Van Zyl [49]. Similarities with Dunn and Van Zyl's theoretical results are not surprising since these authors calculated the cross-section of the process $H_2^+(X, v = 0) + e^- \rightarrow H^+ + H + e^-$ which is close to our 300 K WTCS. The disagreement with Dunn and Van Zyl, Tawara et al. and Mathur et al. experimental values is due to the fact that the cross-sections measured by these authors include dissociative excitation processes which are not taken into account in the present study.

Rate coefficients obtained in this paper are also confronted with previous works. There are no available data for OH and the only accessible values are for the following processes involving H_2:

$$
\begin{aligned}
&H_2(X) + e^- \rightarrow H + H + e^-\\
&H_2(X) + e^- \rightarrow H_2(B) + e^-\\
&H_2(X) + e^- \rightarrow H_2(C) + e^-\\
&H_2(X) + e^- \rightarrow H_2^+(X) + e^- + e^-.
\end{aligned}
$$

As shown in Figures 5 to 8, the agreement between the rate coefficients calculated in this study and those proposed by Janev et al. [23] is acceptable in all cases. There are more discrepancies at low temperature ($T < 10000$ K) for the dissociation of H_2(X) (cf. Fig. 5) with the experimental work of Du and Hessler [24] because the reaction rate determined by these authors corresponds to global dissociation of H_2: $H_2 + M \rightarrow H + H + M$ where M could be any particle of the plasma.

4 Conclusion

Using the WTCS theory, electron impact excitation, ionisation and dissociation cross-sections are calculated for the main electronic states of H_2, OH and their corresponding ions for which spectroscopic molecular constants are available. Reaction rate coefficients are then determined assuming Maxwellian energy distribution functions for electrons and heavy particles. The results obtained are validated by comparison with previous published data. For excitation and ionisation, cross-sections are normalised with experimental values. Due to the lack of data, it was not possible to define normalisation factors for the majority of processes involving OH molecules. It will be consequently suitable to re-evaluate WTCS calculated in the present study if new cross-section measurements concerning OH become available in the future.

Calculations are performed as a function of electrons and heavy particles kinetic temperatures (θ_e and θ_g) and rate coefficients are fitted in an Arrhenius form $k(\theta) = a(\theta^b)\exp(-c/\theta)$ in the one-temperature case. The set of cross-sections obtained in this work is usable for any kind of plasma whereas reaction rates are limited to thermal or quasi thermal plasmas for which the assumption of Maxwellian energy distribution functions are supposed to be valid.

These data are actually used to develop a collisional-radiative model for H_2O vapour with the aim to study the expansion phase of a water LIBS plasma.

The authors gratefully acknowledge the "Comité Mixte Franco-Tunisien pour la Coopération Universitaire (CMCU)" for its support in the present study.

References

1. K. Song, Y.-I. Lee, J. Sneddon, Appl. Spectrosc. Rev. **32**, 183 (1997)
2. R. Knopp, F.J. Scherbaum, J.I. Kim, Fresenius J. Anal. Chem. **355**, 16 (1996)
3. D.A. Cremers, L.J. Radziemski, T.R. Loree, Appl. Spectrosc. **38**, 721 (1984)
4. C. D'Angelo, J. Gomba, D. Iriarte, G. Bertucelli, Proc. SPIE **3572**, 534 (1999)
5. P. Fichet, A. Toussaint, J.F. Wagner, Appl. Phys. A **69**, S591 (1999)
6. G. Arca, A. Ciucci, V. Palleschi, S. Rastelli, E. Tognini, Appl. Spectrosc. **51**, 1102 (1997)
7. G. Arca, A. Ciucci, V. Palleschi, S. Rastelli, E. Tognini, Proc. Int. Goesc. Rem. Sens. Symp. (IGARSS 96) **2**, 854 (1996)
8. G. Arca, A. Ciucci, V. Palleschi, S. Rastelli, E. Tognini, Proc. Int. Goesc. Rem. Sens. Symp. (IGARSS 96) **1**, 520 (1996)
9. V. Yargeau, G. Soucy, M.I. Boulos, Plasma Chem. Plasma Process. **19**, 327 (1999)
10. M. Violier, N. Cerqueira, C. Vandensteendan, J.M. Baronnet, in *Proceedings of the XVth International Conference on Gas Discharges and their Applications*, Toulouse (France) **1**, 745 (2004)
11. G. Colonna, A. Casavola, M. Capitelli, Spectrochim. Acta B **56**, 567 (2001)
12. G. Colonna, L.D. Pietanza, M. Capitelli, Spectrochim. Acta B **56**, 587 (2001)
13. J. Bacri, A. Médani, Physica C **101**, 399 (1980)
14. J. Bacri, A. Médani, Physica C **101**, 410 (1980)
15. J. Bacri, A. Médani, Physica C **112**, 101 (1982)
16. A.M. Gomes, A. Essoltani, J. Bacri, J. Quant. Spec. Radiat. Transfer **43**, 471 (1990)
17. J.P. Sarrette, A.M. Gomes, J. Bacri, C.O. Laux, C.H. Kruger, J. Quant. Spec. Radiat. Transfer **53**, 125 (1995)
18. Ph. Teulet, J.P. Sarrette, A.M. Gomes, J. Quant. Spec. Radiat. Transfer **62**, 549 (1999)
19. H. Deutsch, K. Becker, T.D. Märk, Int. J. Mass. Spectrom. **167/168**, 503 (1997)
20. M. Bobeldijk, W.J. Van der Zande, P.G. Kistemaker, Chem. Phys. **179**, 125 (1994)
21. K.N. Joshipura, M. Vinodkumar, U.M. Patel, J. Phys. B **34**, 509 (2001)
22. V. Tarnovsky, H. Deutsch, K. Becker, J. Chem. Phys. **109**, 932 (1998)
23. R.K. Janev, W.D. Langer, K. Evans, D.E. Post, *Elementary Processes in Hydrogen Helium Plasmas,* (Springer-Verlag, New York, 1987)
24. H. Du, J.P. Hessler, J. Chem. Phys. **96**, 1077 (1992)
25. R. Celiberto, M. Capitelli, N. Durante, U.T. Lamanna, Phys. Rev. A **54**, 432 (1996)
26. S. Chung, C.C. Lin, Phys. Rev. A **17**, 1874 (1978)
27. M.A. Khakoo, S. Trajmar, Phys. Rev. A **34**, 146 (1986)
28. Lee Mu-Tao, R.R. Lucchese, V. McKoy, Phys. Rev. A **26**, 3240 (1982)
29. S.P. Khare, Phys. Rev. **149**, 33 (1966)
30. G.P. Arrighini, F. Biondi, C. Guidotti, A. Biagi, F. Marinelli, Chem. Phys. **52**, 133 (1980)
31. R. Celiberto, T.N. Rescigno, Phys. Rev. A **47**, 1939 (1993)
32. E. Krishnakumar, S.K. Srivastava, J. Phys. B **27**, L251 (1994)
33. D. Rapp, P. Englander-Golden, J. Chem. Phys. **43**, 1464 (1965)
34. H. Deutsch, K. Becker, S. Matt, T.D. Märk, Int. J. Mass. Spectrom. **197**, 37 (2000)
35. H.C. Straub, P. Renault, B.G. Lindsay, K.A. Smith, R.F. Stebbings, Phys. Rev. A **54**, 2146 (1996)
36. V. Dose, P. Pecher, R. Preuss, J. Phys. Chem. Ref. Data **29**, 1157 (2000)
37. H. Tawara, Y. Itikawa, H. Nishimura, M. Yoshino, J. Phys. Chem. Ref. Data **19**, 617 (1990)
38. R. Celiberto, R.K. Janev, A. Laricchiuta, M. Capitelli, J.M. Wadehra, D.E. Atems, At. Data Nucl. Data Tables **77**, 161 (2001)
39. G. Herzberg, *Spectra of diatomic Molecules*, 2nd edn. (Van Nostrand Reinhold, New-York, 1950)
40. K.P. Huber, G. Herzberg, *Molecular Spectra and Molecular structure. IV Constants of Diatomic Molecules* (Van Nostrand Reinhold, New York, 1978)
41. H. Helm, P.C. Cosby, D.L. Huestis, Phys. Rev. A **30**, 851 (1984)
42. R.P. Saxon, B. Liu, J. Chem. Phys. **85**, 2099 (1986)
43. D.R. Yarkony, J. Phys. Chem. **97**, 111 (1993)
44. K.S. Drellishak, D.P. Aeschliman, A. Bulent Cambel, Phys. Fluids **8**, 1590 (1965)
45. E. Gerjuoy, S. Stein, Phys. Rev. **97**, 1671 (1955)
46. H.W. Drawin, *Collision and transport cross-section*, report EUR-CEA-FC-383, Fontenay-aux-roses (1967); H.W. Drawin, *Plasma Diagnostics*, edited by W. Lochte-Holtgreven (North Holland, Amsterdam, 1968)
47. M. Gryzinski, Phys. Rev. **138**, A305 (1965); M. Gryzinski, Phys. Rev. **138**, A336 (1965); M. Gryzinski, Phys. Rev. **115**, 374 (1959); M. Mitchner, C.H. Kruger, *Partially ionized gases* (Wiley, New York, 1973)
48. D. Mathur, J.B. Hasted, S.U. Khan, J. Phys. B **12**, 2043 (1979)
49. G.H. Dunn, B. Van Zyl, Phys. Rev. **154**, 40 (1967)